Applied Mathematical Sciences, Vol. 2, 2008, no. 20, 981 - 993

PDEs-Based Method for Image Enhancement

Ehsan Nadernejad

Department of Computer Engineering, Faculty of Engineering
Mazandaran Institute of Technology
ehsan_nader@yahoo.com

Hamidreza Koohi

Department of Computer Engineering, Faculty of Engineering
Shomal higher-education Institute
P.O. Box: 731, Amol, Iran
koohi@shomal.ac.ir

Hamid Hassanpour

Department of Computer Engineering, Faculty of Engineering
Mazandaran Institute of Technology
ehsan_nader@mit.ac.ir

Abstract

Removing noise from data is often the first step in data analysis. De-noising technique should not be only reduce the noise, but do so without blurring or changing the location of the edges. Many approaches have been proposed to accomplish this; in this paper, we have compared three recently developed techniques for image enhancement and denoising. These methods are based on the use of partial differential equations, including second order, fourth order, and the complex partial differential. We consider various well-known measuring metrics used in image processing applied to standard images in this comparison. In this study, it is shown that the capability of the PDE-based approaches depends highly on the neighboring structure. Our investigations show that in an image where the energy of noise is low, the complex diffusion method offers a better result in image denoising compared to other methods. However, when the energy of the noise increases, performance of the complex diffusion method declines. In general, for the case when the energy of noise in an image is unpredictable, using the heat equation for image denoising is recommended.

Keywords: Complex diffusion, Denoising, Partial differential equation, Image processing

I. INTRODUCTION

Noise reduction is usually the first process that is used in the analysis of digital images. In any image denoising algorithm, it is very important that the denoising process has no blurring effect on the image, and makes no changes or relocation to image edges.

There are various methods for image denoising. Using simple filters, such as average filter, median filter and Gaussian filter, are some of the techniques employed for image denoising [11]. These filters reduce noise at the cost of smoothing the image and hence softening the edges.

To overcome the above-mentioned problems, the partial differential equations (PDEs) –based methods have been introduced in the literature [1,10]. These methods assume the intensity of illumination on edges varies like geometric heat flow in which heat transforms from a warm environment to a cooler one until the temperature of the two environments reaches a balanced point. It was shown that these changes are in the form of a Gaussian function [10]. Consequently, sudden changes in edges might be due to the existence of noise. In fact, an image includes a series of regions in which different regions might have different standard deviations.

The paper is organized as follows: Section 2 briefly describes the PDE-based approaches for image denoising. Section 3 introduces various metrics used for performance measuring algorithms in this paper. The experimental results are provided in Section 4. Finally, the conclusion is given in Section 5.

II. REVIEW THE PDE-BASED IMAGE DENOISING TECHNIQUES

The capability of PDE-based methods in image denoising prompted many researchers to search for an improvement in the technique [1,5]. In this section we introduce three recently developed methods in image denoising.

A. The Second order PDEs

In recent years the second order PDEs are widely used for image enhancement and denoising. Perona and Malik initially proposed the idea [9] which is based on heat diffusion equations. For an image I, the equation can be defined as follows:

$$\frac{\partial I(x,y,t)}{\partial t} = \nabla \cdot (c(x,y,t)\nabla I(x,y,t))$$
$$I(x,y,0) = I_0(x,y) \tag{1}$$

Here ∇ is the gradient operator, $c(x,y,t)$ is the diffusion factor, and $\nabla\cdot$ is the divergence operator. If c has a constant value (independent to x,y,t), the obtained equation is called a diffusion equation with an isotropic diffusion factor. In this case, all points and edges would be smoothed as there is no difference between a pixel on an edge and other pixels. It is obvious that this is not an ideal solution. To resolve this deficiency, the diffusion factor could be considered a function of x and y. Hence, the above equation is changed to a linear and anisotropic equation. If c is dependent on the image, the linear equation would be transformed to a nonlinear equation. This is the idea that was suggested in [16],[6]. In these researches two different equations for the diffusion factor were suggested as shown below:

$$c(x,y,t) = \frac{1}{(1+\frac{|\nabla I|^2}{k^2})} \tag{2}$$

$$c(x,y,t) = \exp(-\frac{|\nabla I|^2}{2k^2}) \tag{3}$$

In the above equations the diffusion factor c changes at different points in the image. For those points where the gradient of the image is large, this factor has a small value. Consequently, the diffusion factor would be small around the edges, hence the edges are preserved from smoothing. In both (2) and (3) k is used to control the diffusion factor.

Equation (1) is considered an efficient tool for noise removal and scale space analysis of images. Although the method is thought to be comparably better than the other methods [15], it tends to cause blocky effects in images. These blocky effects are visually unpleasant and the possibility of detecting them as false edges by edge detection algorithms is high. Several papers [16]-[3] have noted that anisotropic diffusions with diffusion coefficients given by (2) and (3) are ill disposed in the sense that images close to each other are likely to diverge during the diffusion process. In [13] it is noted that even without noise, a stair-casing effect can arise around smooth edges. Since anisotropic diffusion is designed such that smooth areas are diffused faster than less smooth ones, blocky effects will appear in the early stage of diffusion, even though all the blocks will finally merge to form a smoother image. When there is backward diffusion, however, any step image (piecewise level image) is a global minimum of the energy functional, so blocks will appear in the early stage of the diffusion and will remain as such [15].

B. The Fourth order PDEs

In the past few years, a number of authors have proposed fourth order PDEs for edge detection and image denoising with the hope that these methods would perform better than their second order analogues [15,13]. Indeed there are good reasons to consider fourth order equations. Firstly, fourth order linear diffusion dampens oscillations at high frequencies much faster than second order diffusion.

Secondly, there is the possibility of having schemes that include the effects of curvature in the dynamics, thus creating a richer set of functional behaviors. On the other hand, the theory of fourth order nonlinear PDEs are far less developed than their second order analogues. Also such equations do not possess a maximum principle or comparison principle, and the implementation of the equations could thus introduce artificial singularities or other undesirable behavior [5].
In this paper, we implemented and tested the fourth order PDEs proposed in [16] and [6]. For these methods, the fourth order PDEs, uses the L^2 – curvature gradient flow method as below:

$$\frac{\partial I}{\partial t} = -\nabla^2[c(\nabla^2 I)\nabla^2 I] \tag{4}$$

Where ∇^2 is the Laplacian of the image I . Since the Laplacian of an image at a pixel is zero if the image is planar in its neighborhood, these PDEs attempt to remove noise and preserve edges by approximating an observed image with a piecewise planar image. The equation (4) was associated with the following energy functional:

$$E(I) = \int_{\Omega} f(\left|\nabla^2 I\right|)\partial x \partial y \tag{5}$$

Where Ω is the image support and ∇^2 denotes the Laplacian operator. Since $f(\left|\nabla^2 I\right|)$ is an increasing function of $\left|\nabla^2 I\right|$, its global minimum at $\left|\nabla^2 I\right| = 0$. Consequently, the global minimum of $E(I)$ occurs when:

$$\left|\nabla^2 I\right| = 0 \quad for \quad all(x, y) \in \Omega \tag{6}$$

A planar image obviously satisfies (5)[10], hence is a global minimum of E(u). Planar images are the only global minimum of E(u) if :

$$f^{"}(s) \geq 0 \quad for \quad all \quad s \geq 0 \tag{7}$$

Because the cost function E(u) is convex under this condition. Therefore, the evolution of (4) is a process in which the image is increasingly smoothed until it becomes a planar image. But in the case of second order anisotropic diffusion, f"(s) may not be greater than zero, and as a result the image evolves towards a step image and that is why it suffers from blocky effects. So on image processed by fourth order PDEs will look less blocky than that processed by second order anisotropic diffusion.

In [6] two different functions have been proposed to measure the oscillations in the noisy data and is given below:

$$E_1(I) = \int_{\Omega} (\left|I_{xx}\right| + \left|I_{yy}\right|)\partial x \partial y \tag{8}$$

or

$$E_2(I) = \int_{\Omega} \sqrt{\left|I_{xx}\right|^2 + \left|I_{xy}\right|^2 + \left|I_{yx}\right|^2 + \left|I_{yy}\right|^2}\,\partial x \partial y \tag{9}$$

The main difference between the two functions is that E_2 (u) is a rotational invariant while E_1(u) is not. However the implementation with E_1(u) is more simple for higher dimensional problems. Based on the above functions *Lysaker* proposed the following 4th order PDE:

$$\frac{\partial I}{\partial t} = -\left(\frac{I_{xx}}{|I_{xx}|}\right)_{xx} - \left(\frac{I_{yy}}{|I_{yy}|}\right)_{yy} - \alpha(I - I_0) \tag{10}$$

where:

$$\alpha = -\frac{1}{\sigma^2}\int_{\Omega}\left(\frac{I_{xx}}{|I_{xx}|}(I - I_0)_{xx} + \frac{I_{yy}}{|I_{yy}|}(I - I_0)_{yy}\right)\partial x\,\partial y \tag{11}$$

This method offers similar results when compared with the method proposed in [15].

C. The Complex Diffusion

Complex diffusion is a comparatively new method and can be applied for image denoising. This is a generalization of diffusion and free *Schrodinger* equations. In various areas of physics and engineering, it was realized that extending the analysis from the real axis to the complex domain is very helpful, even though the variables and/or quantities of interest are real. Analysis of linear complex diffusion shows that the generalized diffusion has properties of both forward and inverse diffusion [2].

In 1931, *Schrodinger* proposed the possibility of using diffusion theory as a starting point for the derivation of the equations of quantum theory. This idea was developed by *Fuerth* who indicated that the Schrodinger equation could be derived from the diffusion equation by introducing a relation between the diffusion coefficient and *Planck's* constant, and stipulating that the probability amplitude of quantum theory should be given by the resulting differential equation [8]. It has been the goal of a variety of subsequent approaches to derive the probabilistic equations of quantum mechanics from equations involving probabilistic or stochastic processes. Complex diffusion-type processes are encountered in quantum physics and in electro optics. The time dependent Schrodinger equation is the fundamental equation of quantum mechanics [8] . In the simplest case for a particle without spin in an external field it has the form:

$$i\ \eta\frac{\partial \psi}{\partial t} = -\frac{\eta^2}{2m}\Delta\psi + V(x)\psi \tag{12}$$

Where $\psi = \psi(x,t)$ is the wave function of a quantum particle, m is the mass of the particle, η is Planck's constant, V(x) is the external field potential, Δ is the Laplacian and $i = \sqrt{-1}$. With an initial condition $\psi\big|_{t=0} = \psi_0(x)$, requiring that $\psi(0,t) \in L_2$ for each fixed t, the solution is $\psi(0,t) = e^{\frac{-i}{h}tH}\psi_0$, where the exponent is

shorthand for the corresponding power series, and the higher order terms are defined recursively by $H^n\psi = H(H^{n-1}\psi)$. The operator:

$$H = -\frac{\eta^2}{2m}\Delta + V(x) \tag{13}$$

Called the *Schrodinger* operator, is interpreted as the energy operator of the particle under consideration. The first term is the kinetic energy and the second is the potential energy. The duality relations that exist between the Schrodinger equation and the diffusion theory have been studied in [8]. By solving equations (1) and (12) we will get the following two equations:

$$I_{RT} = C_R I_{Rxx} - C_I I_{Ixx}, I_R(x,y,0) = I_0$$
$$I_{IT} = C_I I_{Rxx} + C_R I_{xx}, I_I(x,y,0) = 0 \tag{14}$$

Where I_{RT} is the image obtained for the real plane and I_{IT} is the image obtained for the imaginary plane at time T and $C_R = \cos(\theta), C_I = \sin(\theta)$. The relation $I_{Rxx} \approx \theta I_{Ixx}$ holds for small theta approximation :

$$I_{RT} \approx I_{Rxx}; I_{IT} \approx I_{Ixx} + \theta I_{Rxx} \tag{15}$$

where I_R is controlled by a linear forward diffusion equation, whereas I_I is affected by both the real and imaginary equations. The above-mentioned method is a linear complex diffusion equation. A more efficient nonlinear complex diffusion can be written as in equation (16) :

$$I_t = \nabla.(c(\mathrm{Im}(I)\nabla I) \tag{16}$$

where:

$$c(\mathrm{Im}(I)) = \frac{e^{i\theta}}{1 + \left(\frac{\mathrm{Im}(I)}{k\theta}\right)^2} \tag{17}$$

In the above equation k is the threshold parameter. The phase angle θ should be small ($\theta \approx 1$). Since the imaginary part is normalized by θ, the process is hardly affected by changing the value of θ, as long as it stays small [2].

III. PERFORMANCE METRICS

In this paper four well known metrics are used to evaluate the algorithms, which are introduced here briefly.

A: Figure of Merit Metric

The figure of merit (FOM) the edge preserving measure that is defined as below [14]:

$$FOM = \frac{1}{\max\left\{\hat{N}, N_{ideal}\right\}} \sum_{i=1}^{\hat{N}} \frac{1}{1+d_i^2 \lambda} \tag{18}$$

In this equation $\hat{N}$ and N_{ideal} are the numbers of detected and original edge pixels, respectively; d_i is the Euclidean distance between the ith detected edge pixel and the nearest original edge pixel; λ is a constant typically set to 1/9. The dynamic range of *FOM* is between the processed image and the ideal image. We used the Canny edge detector [17] to find the edge in all processed results.

B: Structural SIMilarity Metric

The structural similarity etric (SSIM) proposed in [18] consists of three different metrics. Let $x = \{x_i \,|\, i = 1,2,3,...,N\}$, $y = \{y_i \,|\, i = 1,2,3,...N\}$ be the original and the test images, respectively. The proposed quality index is defined as:

$$SSIM = Q = \frac{4\sigma_{XY}\bar{X}\bar{Y}}{(\sigma_X^2 + \sigma_Y^2)[(\bar{X})^2 + (\bar{Y})^2]} \tag{19}$$

where:

$$\begin{aligned} &\bar{X} = \frac{1}{N}\sum_{i=1}^{N} x_i \quad , \bar{Y} = \frac{1}{N}\sum_{i=1}^{N} Y_i \\ &\sigma_x^2 = \frac{1}{N-1}\sum_{i=1}^{N}(x_i - \bar{X})^2 \quad , \sigma_y^2 = \frac{1}{N-1}\sum_{i=1}^{N}(y_i - \bar{Y})^2 \\ &\sigma_{xy} = \frac{1}{N-1}\sum_{i=1}^{N}(x_i - \bar{X})(y_i - \bar{Y}) \end{aligned} \tag{20}$$

The dynamic range of *SIMM* is [-1, 1]. The best value 1 is achieved if and only if $y_i = x_i$ for all $i = 1,2,3,...,N$. The lowest value of -1 occurs when $y_i = 2\bar{X} - x_i$ for all $i = 1,2,3,...,N$. This quality index models any distortion as a combination of three different factors: loss of correlation, luminance distortion, and contrast distortion. In order to understand this, we rewrite the definition of Q as a product of three components:

$$\begin{aligned} &SSIM = Q = Q_1 Q_2 Q_3 = \\ &\frac{\sigma_{xy}}{\sigma_x \sigma_y} \times \frac{2\bar{X}\bar{Y}}{(\bar{X})^2 + (\bar{Y})^2} \times \frac{2\sigma_x \sigma_y}{\sigma_x^2 + \sigma_y^2} \\ &= s(x,y)^{\alpha} \times l(x,y)^{\beta} \times c(x,y)^{\gamma} \end{aligned} \tag{21}$$

The first component is the correlation coefficient between x and y, which measures the degree of linear correlation between x and y, and its dynamic range is [-1, 1]. The best value 1 is obtained when $y_i = ax_i + b$ for all $i = 1,2,...,N$, where a and b are constants and $a > 0$. Even if x and y are linearly related, there still

might be relative distortions between them, which are evaluated in the second and third components. The second component, with a value range of [0, 1], measures how much the x and y are close in luminance. It equals 1 if and only if $\overline{X} = \overline{Y}$. σ_x and σ_y can be viewed as an estimate of the contrast of x and y, so the third component measures the similarities between the contrasts of the images. Its range of values is also [0, 1], where the best value 1 is achieved if and only if $\sigma_X = \sigma_Y$. Parameters α, β, γ are used to adjust the significance of each of the three components. This metric can be implemented for an image as below:

$$MSSIM(x, y) = \frac{1}{M}\sum_{j=1}^{M} SSIM(x_j, y_j) \tag{22}$$

where X and Y are the reference and the distorted images respectively, M is the number of local windows in the image, SSIM is the Structural Similarity Index Matrix, x_j and y_j are the image contents at the j^{th} local window.

C. Mean Square Error (MSE) Metric

This metric is frequently used in signal processing and is defined as follows

$$MSE = \frac{1}{NM}\sum_{i=1}^{N}\sum_{j=1}^{M}(I_{orginal}(i, j) - I_{denoised}(i, j))^2 \tag{23}$$

Here, $I_{original}$ is the original image and $I_{denoised}$ is the denoised image. In this metric, the smaller the MSE value, the better is the denoising performance.

D: SNR Metric

The SNR is well known in signal processing like MSE. Its definition is as follows:

$$(SNR)_{db} = 10\log_{10}\left[\frac{\sigma^2_{Signal}}{\sigma^2_{Noise}}\right] \tag{24}$$

Here, when the denoised image has a large SNR it will be closer to the original image and will have a better quality.

IV. EXPERIMENTAL RESULTS

To compare the performance of the above-described techniques in image denoising, they have been implemented using Matlab. Then the algorithms were applied to 100 standard images provided in [4].

To find the numerical solution for the algorithms under comparison, we used two neighboring structures shown in Figure 1 [4].

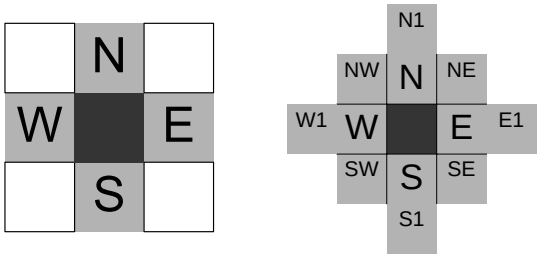

a ***b***

Figure 1. The neighboring structures for numerical solution of PDEs

In these experiments, to make the images noisy, the Gaussian noise and impulse noise have been used with 64 as the average value for both of the noises, and a variance of 400 for the Gaussian noise, respectively. These noises have been added to the images, once separately and then together.

The implemented results on 5 images are shown in Figure 2. As can be seen from the figure, those algorithms that use the neighboring structure shown in Figure 1.b have a better performance.

It may need to be mentioned that in those equations which use the structure shown in Figure 1.a, only horizontal and vertical edges are under consideration. In using this neighboring structure, the edges are considered sharp or sudden. Consequently, a single point is assumed to be the edge, and hence, preserved whereas in a real image the edges have a smooth nature. Therefore the neighboring structure shown in Figure 1.b can have a better performance when considering the smoothly changing structure of edges. The results of the FOM measure shown in Figure 2-a attest that the second neighboring structure has a better performance in preserving edges.

The obtained results using the SSIM measure shown in Figure 2-b indicate that the second neighboring structure offers more similar images to the original images.

Our investigations show that in an image in which the energy of noise is low, the complex diffusion offers a better result in image denoising compared to the other methods. However, when the energy of noise increases, performance of the complex diffusion declines. In general, for the case where the energy of noise in an image is unknown, using the heat equation for image denoising is recommended.

The results of applying different algorithms on one of the images are shown in Figure 3 for visual comparison.

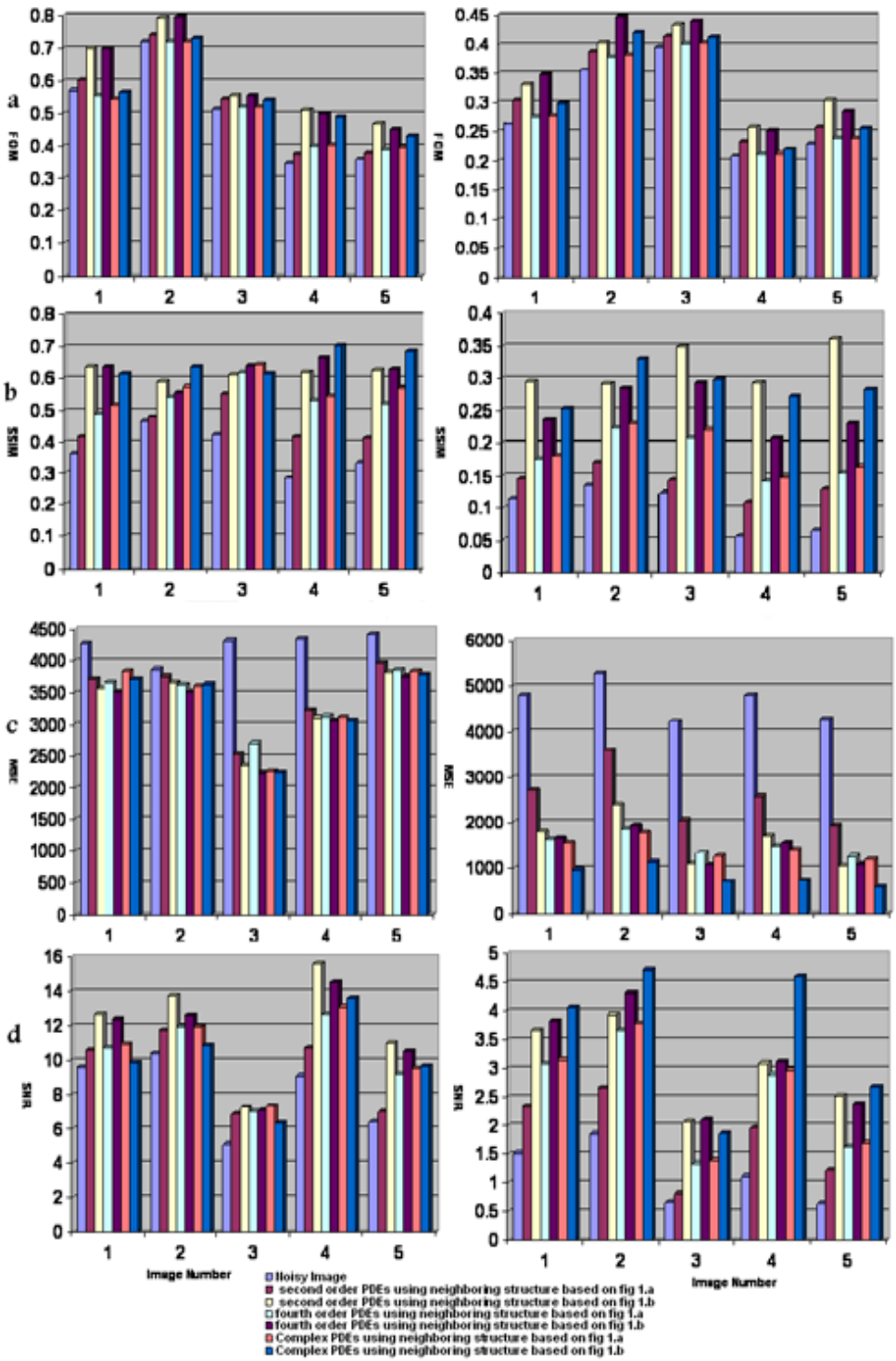

Figure 2. Results of measuring performance of the compared algorithms on 5 different images have shown in Appendix I using: a) FOM, b) SSIM, c) MSE, and d) SNR. (Right chart using Gaussian noise and Left chart using Impulse noise)

Figure 3: the results of using different algorithms respectively from up to down and left to right: original image, noisy image, the rest ones are respectively enhanced from of noisy image by using second order PDEs using neighboring structure based on Figure 1.a, second order PDEs using neighboring structure based on Figure 1.b, fourth order PDEs using neighboring structure based on Figure 1.a, second order PDEs using neighboring structure based on Figure 1.b, Complex PDEs using neighboring structure based on Figure 1.a, Complex PDEs using neighboring structure based on Figure 1.b

V. CONCLUSION

In this research various methods of PDE-based noise reduction have been analyzed. In the analysis, various well-known measuring metrics have been used. The results show that by using the heat equations noise reduction gives a better result compared to other methods. In addition, by using this method the quality of the image is better enhanced.

REFERENCES

[1] B. Fisch and E.L. Schowart, learning an Integral Equation Approximation to Nonlinear Anisotropic Diffusion in Image processing, *Dept. cognitive and Neural Systems Boston University.*

[2] G. Gilboa, N. Sochen and Y.Y. Zeevi, Image Enhancement and Denoising by Complex Diffusion Processes, *IEEE Trans. On Pattern Analysis and Machine Intelligence, Vol. 26, No. 8, 2004.*

[3] G.W. Wei., Generalized Perona-Malik equation for image processing, *IEEE Signal Processing Letters, 6(7), 1999, pp 165–167.*

[4] H. Hassanpour, E. Nadernejad and H. Miar, Image Enhancement Using Diffusion Equations*. ISSPA 2007 Sharjah.*

[5] J.B. Greer and A. L. Bertozzi, Traveling wave solutions of fourth order PDEs for image processing, *SIAM Journal on Mathematical Analysis, vol. 36, no. 1, 2004.*

[6] M. Lysaker, A. Lundervold and X. Tai, Noise removal using fourth order partial differential equation with applications to medical magnetic resonance images in space and time, *IEEE Trans. Image Processing, vol. 12, no. 12, 2003, pp 1579 – 1590.*

[7] M. Lysaker, S. Osher and X. Tai, Noise removal using smoothed normals and surface fitting. *UCLA CAM, 2003.*

[8] M.D. Kostin, Schrodinger-Fuerth quantum diffusion theory: Generalized complex diffusion equation*, J. Math. Phys. 33 (I), 1992*

[9] Perona. P and Malik. J, Scale-space and edge detection using anisotropic diffusion, *IEEE Transactions on Pattern Analysis and Machine Intelligence 12(7), pp. 629–639, 1990.*

[10] Perona. P and Malik. J, Scale-space and edge detection using anisotropic diffusion, *in Proceedings, IEEE Computer Society workshop on Computer Vision, pp. 16–27, 1987*.

[11] R.C. Gonzalez and R. E. Woods, Digital Image Processing, *Prentice Hall 2004*.

[12] R.C. Gonzalez and R.E. Woods, Image Databases
"http://www.imageprocessingplace.com/DIP/dip_image_databases".

[13] T. Chan, A. Marquina, and P. Mulet, High-order total variation based image restoration, *SIAM J. Sci. Comp, 22(2), 2000, pp 503–516.*

[14] W.K. Pratt, Digital Image Processing, *Wiley, New York, NY, USA, 1978.*

[15] Y. You and M. Kaveh, Fourth order partial differential equations for noise removal, *IEEE Trans. Image Processing, vol. 9, no. 10, 2000, pp 1723-1730.*

[16] Y. You, W. Xu, A. Tannenbaum and M. Kaveh, Behavioral analysis of anisotropic diffusion in image processing, *IEEE Trans. Image Processing, vol. 5, no. 11, 1996, pp 1539-1553.*

[17] Y. You and Acton S, Speckle reducing anisotropic diffusion. *IEEE Trans Image Process 2002;11(11):1260–70.*

[18] Z. Wang and A.C. Bovik, A universal image quality index, *IEEE Signal Processing letters, vo.9,no.3,pp-81-84, 2002.*

Received: September 30, 2007